Lab on a Chip

HIGHLIGHT

Research highlights

Imee G. Arcibal,[a] Mehmet R. Dokmeci[bc] and Ali Khademhosseini*[bcde]

DNA structure and sequence mapping in a nanofluidic device

In the ten years since the Human Genome Project was deemed complete, thousands of human genomes have been sequenced,[1] but none to completion. These missing sections in the reference sequence cannot be bridged with the current resolution of next-generation sequencing and cytogenetics, which leave gaps in the mapped structure from the kilobase to megabase range. Furthermore, as more individual genomes are sequenced, person to person variations have come to light with large sequence stretches that do not align with known sequences of the reference genome. These variable regions and their corresponding structural variations (SVs), which include rearrangement, loss, and gain of genomic regions, have been implicated in disease and the appearance of certain phenotypes. Consequently, it is important to not only sequence these stretches of DNA in these variable regions, but also preserve haplotype (set combinations of DNA sequences) and location information.

Techniques, such as single-molecule optical mapping, have previously been employed to examine these regions; however, they do not preserve haplotype nor are the samples recoverable for further analysis. Several lab-on-a-chip systems incorporating nanofluidics have been reported to stretch and map DNA. Unfortunately, these devices have yet to adequately detect SV and require purified DNA.[2,3] Recently, Mir and colleagues[4] have circumvented these issues and designed a platform capable of DNA extraction, stretching, mapping, and recovery. Their design takes advantage of a micro- to nanofluidics interface to load cell extracts directly onto the device, where the stained DNA is denatured and renatured to create a fluorescence pattern before it enters a nanoslit, in which it is stretched and analyzed (Fig. 1). The key aspect of their design was the utilization of hydrodynamic flow and nanoconfinement, which stretched the DNA (up to its 98% length), suppressed longitudinal Brownian motion and enabled mapping of a single molecule.

Marie *et al.*[4] initially employed a well-studied genome to create denaturation–renaturation (DR) maps using their device for comparison with a theoretical DR map created from human reference genome 18 (hg18). Using a previously published algorithm,[5] they were able to correctly identify the origin of 21 molecules (out of 21) randomly picked from those that had been DR mapped. They acknowledge that their 100% success rate in determining the original sequence location within the reference genome involved some luck, as each molecule came from a sequenced portion of the genome. Additional analysis of the DR maps yielded detection of both large (>0.1 Mb) and small (<0.1 Mb) SVs in the generated experimental DR maps when comparing them to maps created from the reference genome.

To further assess the applicability of their platform to analyze an unpredictable sequence, they employed chromosomes from the Jurkat T-cell leukemia line known to exhibit substantial genome instability. DR maps created from these chromosomes were readily observed to have two repetitive elements, which formed a pattern along the length of the DNA molecule. Given their device design, they were able to recover the analyzed DNA and perform additional analyses after amplification. Following next-generation sequencing and fluorescence *in situ* hybridization (FISH), they were able to confirm their identification of the chromosomal origin of the

[a] US Army Corps of Engineers Construction Engineering Research Laboratory, Champaign, Illinois 61822, USA

[b] Center for Biomedical Engineering, Department of Medicine, Brigham and Women's Hospital, Harvard Medical School, Cambridge, Massachusetts 02139, USA. E-mail: alik@rics.bwh.harvard.edu

[c] Harvard-MIT Division of Health Sciences and Technology, Massachusetts Institute of Technology, Cambridge, Massachusetts 02139, USA

[d] Wyss Institute for Biologically Inspired Engineering, Harvard University, Boston, Massachusetts 02115, USA

[e] World Premier International-Advanced Institute for Materials Research (WPI-AIMR), Tohoku University, Sendai 980-8577, Japan

Fig. 1 A fluidic platform for DR mapping and SV detection in a single DNA molecule. (a) Cell extract is loaded onto the chip and the DNA is partially denatured and renatured to create a DR map. (b) Inlet ports shown in (a) connect to microchannels for DNA handling, which lead to a 85 nm nanoslit that confines and elongates a single DNA molecule. Figure adapted and reprinted with permission from Marie *et al.*[4]

molecule based on the generated DR map, as well as assess whether they had analyzed a single haplotype.

The fluidic platform designed by Marie *et al.* provides several advantages over current state-of-the-art sequencing technologies, which include low potential for DNA loss, straightforward analysis workflow, low-cost device fabrication, and a process amenable to automation. Moreover, the reconciliation of a single molecule at the sequence level and at the cytogenetic level may permit a greater understanding of the role the molecule plays in the hierarchy of the cell, ranging from gene structure to cell function. Future analysis of chromosomal DNA could yield single-molecule genomic maps to enable characterization of cellular heterogeneity within solid tumors and examination of rare cells from biological samples. Characterization at this level has implications for identifying novel drug targets, as well as discovery of new mutations that cause unforeseen phenotypic variations.

A microfluidic tissue processor for biomarker detection

Immunohistochemical analysis is a cornerstone of clinical pathology with biomarker expression playing a vital role in cancer diagnosis, prognosis, and treatment regimens. Analyses involving immunohistochemistry (IHC) are often qualitative, examining only the presence or absence of a certain protein within a tissue or cell type. Certain applications, however, require more quantitative analysis of protein expression, where the intensity of an observed IHC signal has important implications for potential treatment options. Expression of human epidermal growth factor receptor 2 (HER2) in invasive breast carcinoma is one such case. HER2, a transmembrane tyrosine kinase associated with an aggressive form of breast cancer, connotes adverse prognostic information for breast cancer patients[6] and serves as a target for personalized treatment.[7]

Currently, a combination of IHC and *in situ* hybridization are employed for diagnosis to examine protein expression and gene amplification, respectively. Tissue samples are initially analyzed with IHC and scored on a continuous scale from negative (0), faint (+), intermediate (++), and positive (+++) based on the observed extent of membrane staining. However, the signal obtained from IHC is not proportional to the degree of HER2 expression, yielding some ambiguity in scoring between intermediate and positive scores. This ambiguity is due to the long incubation times (30 min to hours) required for uniform exposure to primary and secondary antibodies, which in turn yields significant adsorption and nonspecific binding of antibodies.

Previous microfluidics approaches have targeted decreasing reagent diffusion times, improving fluidic exchange, reducing analysis times, and multiplexing parallel analyses; however, these platforms were unable to increase the accuracy of the quantitative biomarker expression analysis and thus have no fix for ambiguous results. Ciftlik *et al.*[8] have recently designed
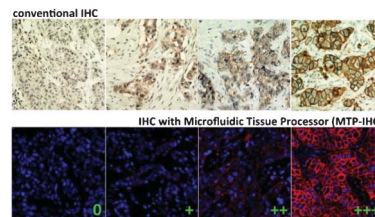
Fig. 2 Representative images of conventional IHC with chromogenic detection (upper) and MTP-IHC with fluorescent detection (lower). Values shown in green correspond to the diagnostic scores; negative (0), faint (+), intermediate (++), and positive (+++), which relate to the amount of membrane staining in the image. Figure adapted and reprinted with permission from Ciftlik *et al.*[8]

a microfluidic tissue processor (MTP) that is automated for IHC biomarker analysis of tissue sections fixed on standard microscope slides. To reduce the total analysis time, the researchers utilized a glass/silicon device that could handle high pressures and permitted high fluid exchange speeds. The MTP permits accurate and reproducible biomarker quantification quickly (<5 min) by exploiting ultra-fast and uniform fluidic exchange within the device.

Gijs and co-workers[8] initially used their device to examine invasive ductal breast carcinomas known to be HER2-positive to validate their antibody exposure protocol and determine primary and secondary antibody incubation times within the MTP. Subsequently, they examined an additional 76 tumor sections with a varying range of HER2 expression using a scanning fluorescence microscope. The corresponding fluorescent signals from these sections were then statistically analyzed and scored in a blinded fashion with no prior knowledge of the original expression score. As shown in Fig. 2, representative images of tissues stained with MTP-IHC protocol could be more easily scored than those analyzed with conventional IHC (more intense cell membrane staining corresponds to higher scores). Analysis with MTP yielded no false-positive or false-negative results and samples with a sub-optimal fluorescent signal could be quickly re-examined on the platform. Moreover, when comparing scores between MTP and conventional IHC for the same samples, the MTP analysis decreased the number of ambiguous results from 27 to 3, reducing the need for further examination of the tissues with *in situ* hybridization.

The MTP platform described by Ciftlik *et al.* could accurately generate stained tissue samples in under 5 min without sacrificing uniform antibody exposure and detection sensitivity. In addition to time savings, the MTP reduced non-specific binding and adsorption of excess antibodies, which in turn permitted the IHC signal to remain proportional to the HER2 concentration within the tissue. Use of this device has a number of implications in the basic science and clinical realms. From a basic science perspective, the MTP system can yield greater fundamental understanding about how the expression of certain biomarkers correlates to disease progression. Moreover, due to the ability to correlate protein levels with the measured signal, treatments could be better tailored

for patients having elevated biomarker levels. The ability to conduct more sensitive analysis of tissue sections also offers an opportunity to identify drug targets and biomarkers for novel treatment strategies.

Fig. 3 SAFI spatiotemporal plots displaying five distinct ion zones under anionic ITP with SPQ (a) and SAB (b) dyes. Figure adapted and reprinted with permission from the Royal Society of Chemistry from Shkolnikov et al.[11]

Microfluidic full field imaging of multiple chemical species concentrations

During the past three decades many researchers have designed and employed microfluidic devices for chemical analysis.[9] Due to the dynamic nature of fluid flow and species interaction in these devices, it is necessary to visualize the full channel and quantify species concentrations to validate and optimize these systems. Luminescence-based visualization techniques, such as photobleaching, phosphorescence, and caged fluorescence[10] have often been utilized to interrogate flow in microfluidic channels; however, they only provide information about the fluorescent molecules themselves and not about other species in the solution. Moreover, these molecules are typically electrically non-neutral and subject to changes in their movement due to local fluid velocity and electric fields.

In attempts to rectify the shortcomings of these other techniques, Shkolnikov and Santiago[11] have developed a novel method to simultaneously visualize and monitor spatiotemporal variations of multiple species concentrations in microflows. The method, species-altered fluorescence imaging (SAFI), employs electrically neutral dyes and provides non-invasive scalar-field quantitation of multiple species concentration fields in two dimensions. Dyes amenable to SAFI must meet multiple criteria, including: net neutrality at the pH of interest, negligible reactivity with the species of interest in the analysis or the microfluidic substrate surface, and high quantum yield and high solubility in the chosen solvent and pH. Additionally, the dye should be part of an analyte-dye pair that has fluorescence that is strongly quenched or enhanced by species of interest. The authors relied primarily on pairs that exhibited Stern–Volmer (collisional) quenching due to their calibration friendly relationship between the analyte concentration and the dye fluorescence.

The authors chose two UV excitable dyes, 6-methoxy-N-(3-sulfopropyl)quinolium (SPQ) and 10-(3-sulfopropyl)acridinium betaine (SAB), to examine their utility for visualization and quantitation in both isotachophoresis (ITP) and electrokinetic instability (EKI) flow experiments. After conducting preliminary calibration experiments and obtaining quenching constants for their buffer solutions, they employed commercially available glass microfluidic chips to observe the migration of five buffer species in ITP. ITP is a technique typically used to preconcentrate and separate analytes, where all ions migrate at the same velocity, but occupy discrete zones due to differences in the electrophoretic mobilities between the ions in the leading and trailing electrolytes. SPQ fluorescence was found to closely fit the Stern–Volmer equation, and thus likely to undergo the expected analyte pair quenching in cationic ITP. SAB, however, did not align with the Stern–Volmer
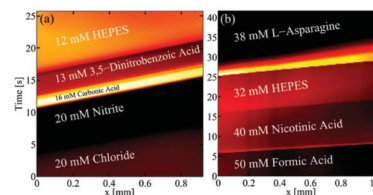
equation, but rather demonstrated fluorescent enhancement within the microchannel. Despite their different interactions with the buffer species, both dyes were able to clearly visualize the interfaces between the different ion zones and quantify background ion densities. The dyes were also examined with anionic ITP, which yielded simultaneous visualization of five distinct ion zones for SPQ and SAB (Fig. 3).

Shkolnikov and Santiago also examined the effects of convective EKI on flow with SPQ. The EKI set-up consisted of a focused high conductivity stream created by electroosmotic flow surrounded by two sheath flows that was perturbed by a perpendicular stream of low conductivity solution, which has previously been shown to create flow instabilities within microchannels.[12] SPQ was able to quantify the concentrations of the ions in the complete flow field for all streams. The dye was also able to capture the transverse velocity fluctuations of the perpendicular flow and allowed for two-dimensional quantitation of local ion densities as the instability mixed the center stream with the surrounding sheath flows.

The SAFI method provides simple visualization of flow channel dynamics, in addition to collectively quantifying ion concentration shock velocities, measuring the concentrations of five species simultaneously, and quantifying the development of an unsteady, chaotic, 2D flow. While the authors acknowledge that the availability of the dyes amenable for SAFI visualization limits the utility of the technique, they do provide a list of 35 potential dye candidates that offer multiple options for a range of pH values and solvent compatibilities. Future use of this technique will enable greater understanding of complex and dynamic fluid flow to facilitate the design of new geometries for fluidics and potentially lead to new analysis and separation techniques.

References

1 G. R. Abecasis, D. Altshuler, A. Auton, L. D. Brooks, R. M. Durbin, R. A. Gibbs, M. E. Hurles and G. A. McVean, *Nature*, 2010, **467**, 1061.

2 S. L. Levy and H. G. Craighead, *Chem. Soc. Rev.*, 2010, **39**, 1133–1152.

3 E. T. Lam, A. Hastie, C. Lin, D. Ehrlich, S. K. Das, M. D. Austin, P. Deshpande, H. Cao, N. Nagarajan, M. Xiao and P. Y. Kwok, *Nat. Biotechnol.*, 2012, **30**, 771–776.

4 R. Marie, J. N. Pedersen, D. L. V. Bauer, K. H. Rasmussen, M. Yusuf, E. Volpi, H. Flyvbjerg, A. Kristensen and K. U. Mir, *Proc. Natl. Acad. Sci. U. S. A.*, 2013, **110**, 4893–4898.

5 W. Reisner, N. B. Larsen, A. Silahtaroglu, A. Kristensen, N. Tommerup, J. O. Tegenfeldt and H. Flyvbjerg, *Proc. Natl. Acad. Sci. U. S. A.*, 2010, **107**, 13294–13299.

6 D. J. Slamon, G. M. Clark, S. G. Wong, W. J. Levin, A. Ullrich and W. L. McGuire, *Science*, 1987, **235**, 177–182.

7 D. J. Slamon, B. Leyland-Jones, S. Shak, H. Fuchs, V. Paton, A. Bajamonde, T. Fleming, W. Eiermann, J. Wolter, M. Pegram, J. Baselga and L. Norton, *N. Engl. J. Med.*, 2001, **344**, 783–792.

8 A. T. Ciftlik, H.-A. Lehr and M. A. M. Gijs, *Proc. Natl. Acad. Sci. U. S. A.*, 2013, **110**, 5363–5368.

9 A. Manz, N. Graber and H. M. Widmer, *Sens. Actuators, B*, 1990, **1**, 244–248.

10 D. Sinton, *Microfluid. Nanofluid.*, 2004, **1**, 2–21.

11 V. Shkolnikov and J. G. Santiago, *Lab Chip*, 2013, **13**, 1632–1643.

12 J. D. Posner, C. L. Pérez and J. G. Santiago, *Proc. Natl. Acad. Sci. U. S. A.*, 2012, **109**, 14353–14356.